Materials Transactions, Vol. 50, No. 10 (2009) pp. 2378 to 2383

Microstructures and Mechanical Properties in Friction Stir Zone of Thixo-Molded AS41 Mg Alloy

Lina Yu[1,*], Kazuhiro Nakata[2] and Jinsun Liao[3]

[1]*Division of Materials and Manufacturing Science, Osaka University, Suita 565-0871, Japan*
[2]*Joining and Welding Research Institute, Osaka University, Ibaraki 567-0047, Japan*
[3]*Kurimoto, Ltd., Osaka 550-8580, Japan*

The friction stir weldability of thixo-molded AS41 Mg alloy was investigated, and the microstructures and mechanical properties in friction stir zones were examined and evaluated. The non-destructive inspection by means of X-ray radiography shows that the optimum FSW condition range of AS41 alloy exists between AZ61 and AE42 alloys, and it seems that the optimum welding condition range increases with decreasing Al content in the Mg alloys. There are mainly three kinds of compounds, i.e. Mg_2Si, MnSi and $Al_{12}Mg_{17}$, in the thixo-molded AS41 base metal, while only two kinds of compounds are found in SZ except $Al_{12}Mg_{17}$ phase. This is because of the decomposition of $Al_{12}Mg_{17}$ phase at the higher temperature caused by the FSW heat input. Furthermore, the average diameter of compounds in SZ decreases with increasing the traveling speed at constant rotation speed due to less heat input. The hardness in SZ is higher than that in BM, and tensile strength and elongation are both improved after welding because the stirring refines and uniforms the microstructure and intermetallic compounds.
[doi:10.2320/matertrans.M2009122]

(Received April 7, 2009; Accepted July 8, 2009; Published September 2, 2009)

Keywords: *microstructure, mechanical property, friction stir welding (FSW), AS41 Mg alloy, thixo-molded*

1. Introduction

Magnesium alloys have many attractive properties, such as high specific strength, lightweight, good castability, and excellent recyclability. It is predicted that the application of magnesium alloys will grow rapidly in the near future, especially in the automotive and aerospace industries.[1–3] With their increasing demand of industrial application, it is necessary to develop effective welding techniques for the joining of Mg alloys. However, fusion welding of these materials is difficult due to the formation of porosity. Friction stir welding (FSW), a novel solid joining technology, is a potential candidate because of its many advantages as compared with the traditional fusion welding processes.[4–10] It can produce pore-free joints, since pores caused by metal solidification are eliminated.[7,8] FSW is called as "green" technology, because it is environmental-friendly and neither shielding gas nor consumable material is required. Furthermore, FSW also has many metallurgical benefits, such as fine microstructures, absence of cracking and defects and so on.[9,10]

In previous studies, FSW of Mg alloys is mainly focused on the die-cast and extruded AZ alloys and AM alloys.[11–14] There is few research works about the AS41 alloy, a heat-resistant alloy with superior creep resistance resulted from the existence of stable intermetallic compounds with high decomposition temperatures at grain boundaries. Due to the precipitation of Si-rich phases,[15,16] AS41 alloy has remarkably higher creep resistance than that of AZ91 and AM60 alloys at higher temperature. In the present work, the thixo-molded AS41 Mg alloy was friction stir welded, and the microstructure and mechanical properties after FSW were extensively investigated.

*Corresponding author, E-mail: yuxueer33@hotmail.com

Table 1 Chemical composition of thixo-molded AS41 Mg alloy.

Alloy	Chemical compositions (mass%)						
	Al	Si	Mn	Cu	Ni	Fe	Mg
AS41	4.48	0.87	0.42	0.0015	<0.0005	0.0066	Bal.

Table 2 FSW parameters.

Load	7.35∼9.8 kN
Tool rotation speed	1000∼1500 rpm
Traveling speed	250∼1000 mm/min

Table 3 Conditions of the tool.

Material of tool	SKD61
Diameter of shoulder	15 mm
Diameter of probe	M5
Length of probe	4.9 mm
Taper angle of shoulder	3°

2. Experimental Procedures

The material used in present study was heat resistant AS41 alloy sheets, which were semi-solid injection cast by thixo-molding. The chemical compositions of the AS41 alloy are given in Table 1. The sheet was 150 mm × 90 mm × 5 mm in specimen size, and the surface was degreased with acetone before welding. Stir-in-plate welding was performed using a load-controlled type FSW machine. The welding parameters and tool's details are shown in Tables 2 and 3, respectively. The tool rotation speed was changed from 1000 to 1500 rpm, and the traveling speed was ranged from 250 to 1000 mm/min.

After welding, the welded joints were examined by X-ray radiography, and the metallurgical inspections were performed on the cross-section of the joints. The metallographic specimens were first mechanically polished and then etched with the solution containing 20 ml acetic acid, 60 ml ethylene glycol, 1 ml nitric acid and 20 ml water. The microstructures of the welded specimens were observed with the optical microscope (OM) and the scanning electron microscope (SEM). Furthermore, X-Ray Diffraction (XRD) was also used to identify the phases in both base metal (BM) and stir zone (SZ). In order to examine the microstructure in the SZ in detail, the size of intermetallic particles in SZ was statistically determined using an image processing method (Image-Pro Plus ver. 4.0).

The hardness measurement was performed on the metallographic specimens crossing the joints at mid thickness. Tensile specimens of 2 mm in thickness were sampled from the SZ and BM along the welding direction, and the top and bottom surfaces were eliminated. Furthermore, the fracture surfaces after the tensile test were examined by SEM.

3. Results and Discussion

3.1 Optimum FSW condition range of thixo-molded AS41 alloy

On the basis of the results of X-ray radiography, the optimum FSW condition range (without any defect) of thixo-molded AS41 alloy is obtained. Figure 1 shows the optimum FSW condition range of the thixo-molded AS41 alloy, together with those of four other kinds of Mg alloys, AZ91D, AZ61, AZ31 and AE42, which are reported in Refs. 17, 18). Among the five kinds of Mg alloys, the optimum condition ranges of AZ91D and AZ61 alloys are relatively narrow, indicating that they cannot be welded with too fast traveling speed, while the welding ranges of AE42 and AZ31 alloys are much wider. The optimum FSW welding range of thixo-molded AS41 alloy exists between AZ61 and AE42 alloys. It seems that the optimum condition range is related to the Al content in Mg alloys. The lower Al content is beneficial to FSW because the high content of Al may result in the decrease of plastic deformability, though it can increase the strength of Mg alloy.

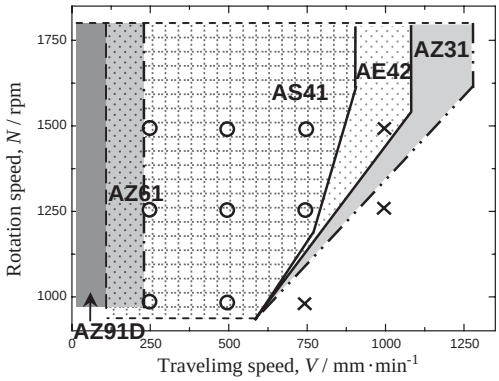

Fig. 1 Appropriate FSW condition range of several kinds of Mg alloys (○, defect-free; ×, defect).

3.2 Microstructures in friction stir welded joint

Figure 2(a) illustrates the overview of the cross-section of thixo-molded AS41 alloy welded with the rotation speed of 1250 rpm and the traveling speed of 250 mm/min, and the microstructures at BM, TMAZ (Thermo-mechanically affected zone) and SZ are given in Fig. 2(b)–(d), respectively. The BM exhibits a typical solidification structure formed in the casting process, having a dendritic microstructure with α-Mg phase and eutectic phase. Grains in the TMAZ have been deformed greatly after stirring due to the heat effect and mechanical deformation, and exhibit obvious arrangement along the metal-flow direction induced by stirring. The SZ contains a fine recrystallized structure instead of dendritic one, and the intermetallic particles (dark phase in Fig. 2) are uniformly dispersed in the SZ. It should be pointed out that the grain boundaries at SZ are hardly revealed with the ordinary metallographic techniques because of too many uniformly-dispersed intermetallic particles, which are preferentially etched. However, the grain structures at SZ can be observed with a help of electron backscattering diffraction (EBSD) technique or transmission electron microscopy (TEM), and the fine recrystallized structures at SZ have been confirmed by using EBSD technique in the present study.

According to the EDX analysis, as shown in Fig. 3, there are mainly three kinds of compounds in the BM of

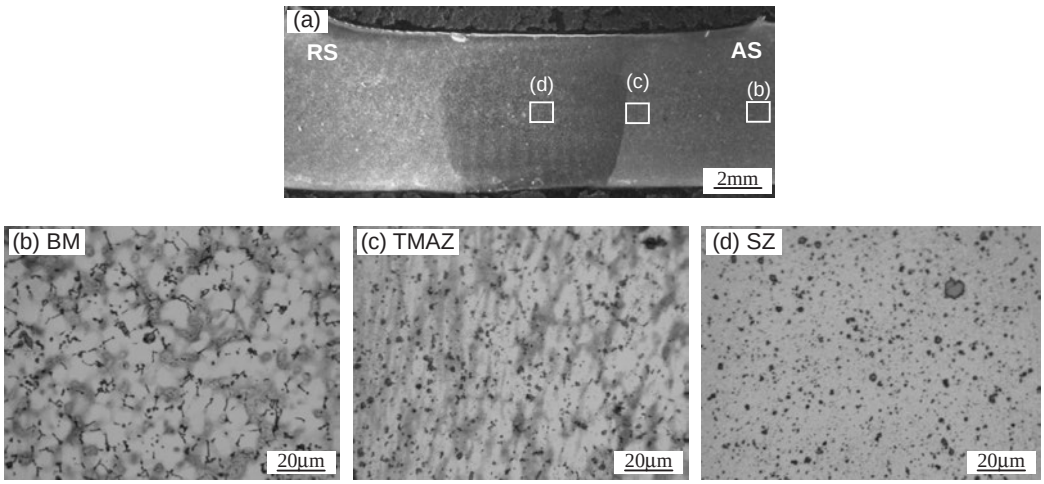

Fig. 2 Macro and micro structures of AS41 alloy FS-welded with the rotation speed of 1250 rpm at the traveling speed of 250 mm/min.

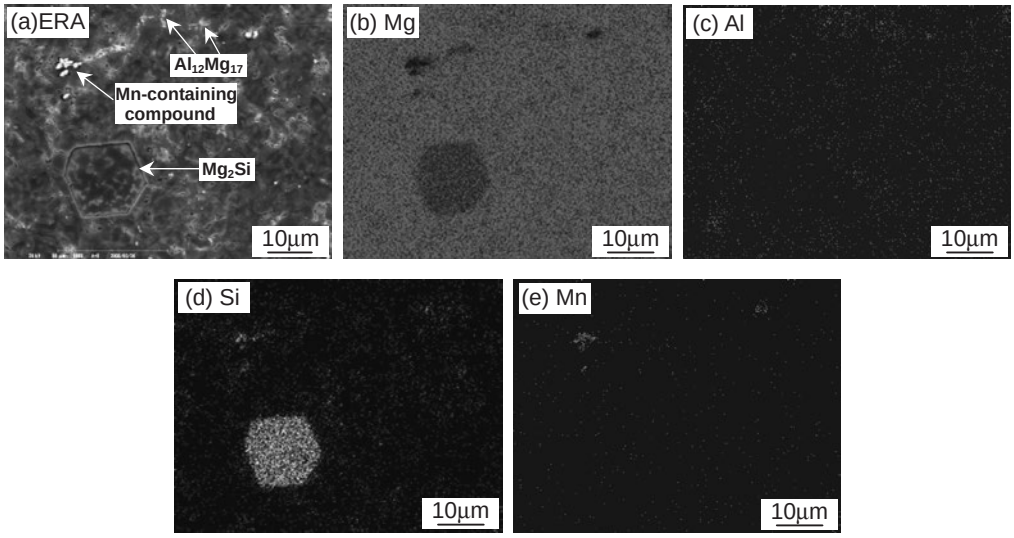

Fig. 3 SEM map analysis of the base metal of the thixo-molded AS41 alloy.

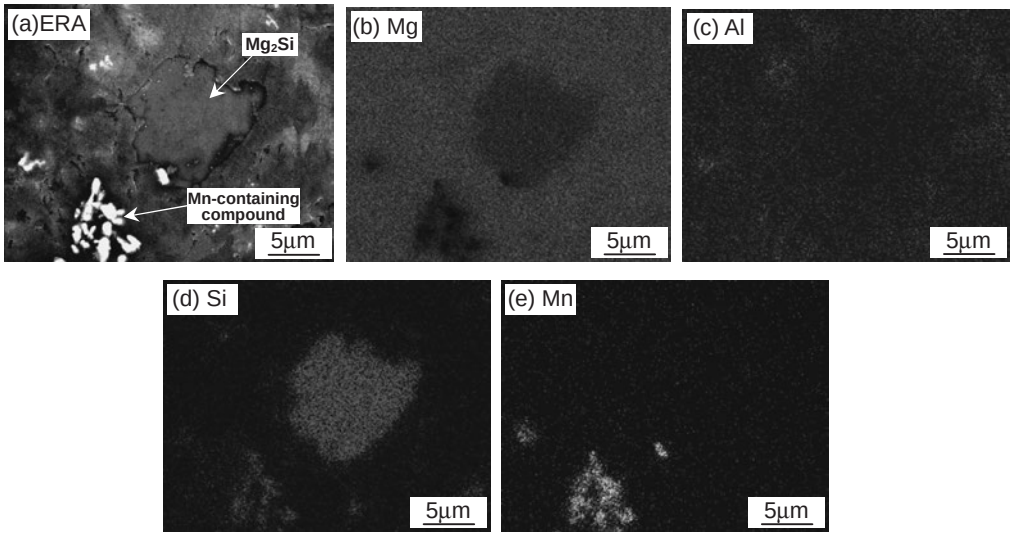

Fig. 4 SEM map analysis of SZ of the thixo-molded AS41 alloy.

thixo-molded AS41 alloy. The big dark compound with regular grainy morphology mainly contains Mg and Si elements, and thus it may be Mg_2Si. The bright small particles, which always congregate together, consist primarily of Mn element and a little of Si element, so that it is a kind of Mn-containing compound. The compounds distributed at the grain boundaries mainly contain Al and Mg elements, which suggest that it is probably $Al_{12}Mg_{17}$ compound (β-phase).

In SZ as illustrated in Fig. 4, the edge of big dark grainy Mg_2Si particles has become more smooth and slick, which was caused by the friction in the stirring process, but they still keep the similar morphology with that in the BM. Similarly, most of the bright small Mn-containing compounds still congregate with each other just like that in BM, and are hardly separated alone in the matrix by FSW. However, the $Al_{12}Mg_{17}$ β-phase seems to have disappeared after stirring. The $Al_{12}Mg_{17}$ β-phase is probably decomposed because the temperature in SZ becomes higher than its decomposition temperature during the stirring process.

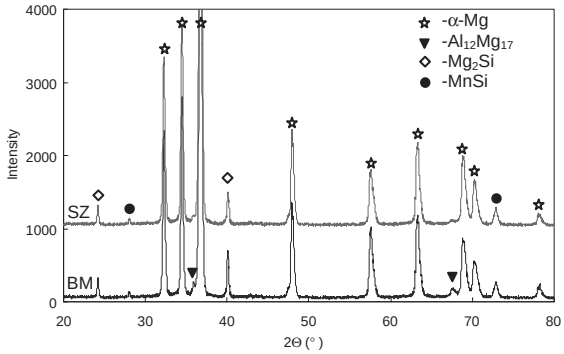

Fig. 5 XRD patterns of SZ and BM in AS41 alloy.

In order to further identify the phases described above, XRD was used to check the samples in BM and SZ. In the XRD patterns presented in Fig. 5, the $Al_{12}Mg_{17}$ β-phase diffraction peaks are obvious in BM of thixo-molded AS41, which shows that the $Al_{12}Mg_{17}$ β-phase exists in the BM. However, the diffraction peak intensity of $Al_{12}Mg_{17}$ β-phase

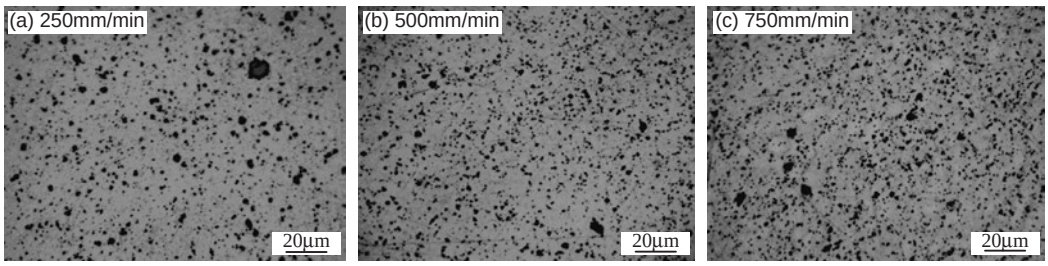

Fig. 6 Microstructures in SZ of AS41 alloys FS-welded with different traveling speeds at constant rotation speed of 1250 rpm.

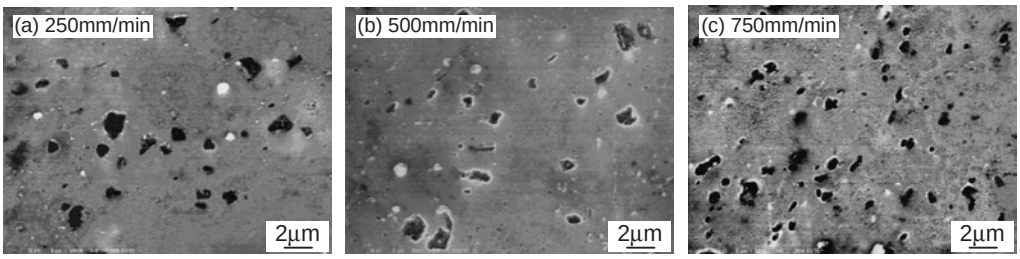

Fig. 7 SEM images with high magnification in SZ of AS41 alloys FS-welded with different traveling speeds at constant rotation speed of 1250 rpm.

in the SZ decreases remarkably, which indicates that the FSW has a great influence on $Al_{12}Mg_{17}$ β-phase, i.e. FSW makes $Al_{12}Mg_{17}$ β-phase decomposed in the SZ. This result is coincident with the SEM results shown in Figs. 3 and 4. In addition, the Mn-containing compound may be MnSi phase, according to the XRD pattern. The above microstructure observation and analysis suggest that, (1) three types of intermetallic phases exist in the thixo-molded AS41 base metal, i.e. grainy Mg_2Si, bright MnSi and $Al_{12}Mg_{17}$ β-phase distributed at grain boundaries, and (2) after FSW, the Mg_2Si and MnSi compounds remain in the SZ, and the grainy Mg_2Si phase and congregated MnSi particles keep their original morphologies, while the edge of Mg_2Si phase becomes more smooth and slick.

According to Mg-Al binary phase diagram,[19] the solid solubility of Al element in Mg matrix is larger than 4.48 mass% when the temperature is higher than 255°C. Under the present welding conditions (rotation speed of 1250 rpm and travelling speed of 250–750 mm/min), the temperature of the samples during FSW is about 430°C,[20] much higher than 255°C, therefore, the solution of Al element into Mg matrix may occur in the stirring process. This explains why there is nearly no $Al_{12}Mg_{17}$ β-phase in the SZ.

3.3 Effect of welding parameters on the microstructure in SZ

The microstructures in SZ welded at various traveling speeds with a constant rotation speed of 1250 rpm are shown in Fig. 6, and the SEM images of SZ with high magnification presented in Fig. 7. The SEM images clearly reveal that the dark Mg_2Si and bright MnSi compounds are included in SZ. The recrystallized structure in SZ changes with welding conditions. At the lower traveling speed of 250 mm/min, the size of the intermetallic compounds is a little bigger, and it seems to decrease with increasing the traveling speed. This result is considered to be caused by different weld heat input, and will be discussed later in detail. Besides, the intermetallic compounds seem to distribute with more obvious arrangement along the stirring-induced metal-flow direction, as the traveling speed is increased.

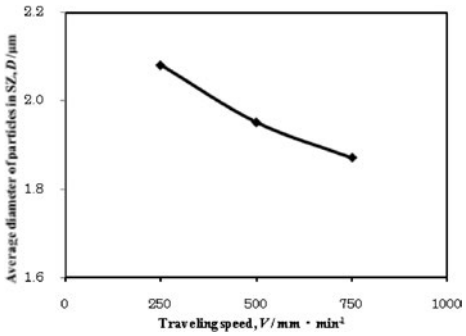

Fig. 8 Relation between average diameter of particles in SZ and traveling speed at the constant rotation speed of 1250 rpm.

Figure 8 illustrates the relation between the average diameter of the intermetallic compounds in SZ and the traveling speed at the constant rotation speed of 1250 rpm. It can be found that the average diameter of the intermetallic compounds in SZ remarkably decreases with increasing the traveling speed from 250 to 750 mm/min. This is because there is less heat input for the intermetallic compound to grow up during FSW at a higher traveling speed.

Heat input introduced by FSW is quite important to the microstructure and the mechanical properties in SZ. Frigaard *et al.*[21] have suggested the following equation for describing the heat input during the FSW:

$$q = \frac{4}{3}\pi^2 \mu P N R^3 \quad (1)$$

where q is the heat input, μ is the friction coefficient, P is the pressure, N is the rotation speed and R is the radius of the

shoulder. For the moving welding, the heat input per unit length, Q, should be considered, so that Kim *et al.*[22] have derived eq. (2) from eq. (1):

$$Q = \frac{\alpha q}{V} = \frac{4}{3}\pi^2 \frac{\alpha \mu PNR^3}{V} \tag{2}$$

where α is the heat input efficiency, and V is the traveling speed. When α, μ and R are assumed to be constant, eq. (3)[22] can be derived from eq. (2):

$$Q \propto \frac{PN}{V} = P \cdot a \propto F \cdot a \tag{3}$$

where a is the ratio of the traveling speed versus the rotation speed, and F is the tool plunge down force.

According to eq. (3), if the rotation speed N is kept constant, the heat input Q increases linearly with decreasing the traveling speed V. At the lower traveling speed (250 mm/min), there is more heat input Q, so the temperature of SZ is relatively higher. Therefore, the intermetallic compounds in SZ will grow up in the welding process due to more heat generation, thus the average diameter of the intermetallic compounds is bigger. Nevertheless, at the higher traveling speed (750 mm/min), because of the less heat input Q, there is no enough heat for the intermetallic compounds to grow up. This explains that the average diameter of the intermetallic compounds in SZ decreases with increasing the traveling speed, as shown in Fig. 6.

3.4 Mechanical properties in SZ

The hardness was measured at mid-thickness across SZ at different traveling speeds with the constant rotation speed of 1250 rpm, as shown in Fig. 9. The hardness of SZ is evidently higher than that of BM, and the average hardness increases from 70 Hv in BM to 77 Hv in SZ, with the increment of 10%, which implies that the mechanical properties can be modified by FSW. Furthermore, the average hardness in SZ increases slightly with traveling speed at the constant rotation speed, i.e. with decreasing welding heat input.

The tensile strength and elongation of specimens machined from BM and SZs at various traveling speeds and a constant rotation (1250 rpm) are presented in Fig. 10. At all traveling speeds in the present study, both the tensile strength and elongation of SZ are higher than those of BM. For example, at traveling speed of 250 mm/min, the tensile strength of SZ is 193 MPa, higher than that of BM, 181 MPa; the elongation of SZ is 6.3%, remarkably higher than that of BM, 4.0%, and the increment is as high as 58%. However, the tensile strength and elongation of SZ decrease with increasing the traveling speed. This is because there are many micro-porosity in the thixo-molded AS41 Mg alloy, and the FSW cannot completely eliminate micro-porosity, especially at higher traveling speeds. That is to say, more micro-porosities or defects may remain in SZ at higher traveling speeds. As compared with BM, however, both the tensile strength and elongation are improved after FSW. The results of tensile test as well as hardness measurement indicate that the mechanical properties have been improved after FSW, which are caused by the finer and uniform microstructure in SZ.

The SEM images of fracture surfaces of BM and SZ tensile specimens are shown in Fig. 11. At the low magnification

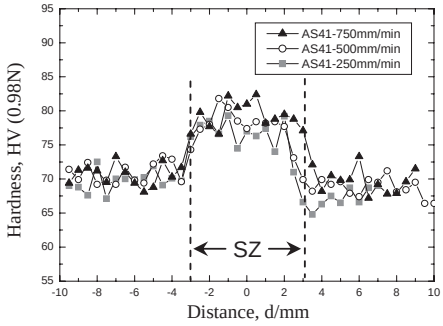

Fig. 9 Hardness of the cross-section of AS41 alloys FS-welded at different traveling speeds with constant rotation speed of 1250 rpm.

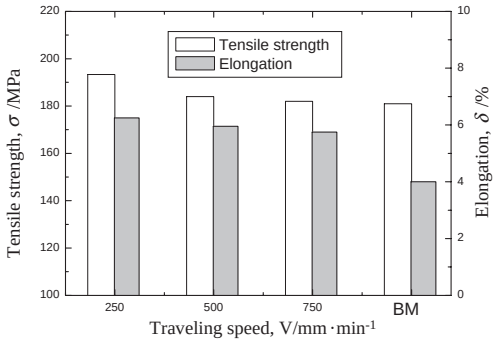

Fig. 10 Tensile strength and elongation of BM and SZ samples FS-welded with 1250 rpm rotation speed at different traveling speeds.

as shown in Fig. 11(a)–(b), solidification defects such as porosity can be easily found on the fracture surface of BM, while there is no obvious defect on the fracture surface of SZ. At high magnification as presented in Fig. 11(c)–(d), it can be seen that the fracture surface of BM contains coarse microstructure besides the porosity defect; however, the fracture surface of SZ exhibits small dimples, which probably result from the homogeneous microstructure of fine grains. It can be concluded from the above results that FSW is a very useful modification method for the mechanical property improvement, because it refines and uniforms the microstructure and intermetallic compounds.

4. Conclusions

Thixo-molded AS41 Mg alloy was friction stir welded, and the microstructures and mechanical properties in SZ were extensively investigated. The following conclusions can be drawn.

(1) According to the X-ray radiography, the optimum FSW condition range of AS41 alloy is obtained, which exists between AZ61 and AE42 alloys. It seems that the optimum FSW condition range widens with decreasing the Al content in the Mg alloys.

(2) There are mainly three kinds of compounds in the thixo-molded AS41 base metal, while after FSW only two kinds of compounds still remain in SZ. The $Al_{12}Mg_{17}$ phase is decomposed during the FSW because the temperature in SZ caused by FSW is higher than its decomposition temperature. The average diameter of intermetallic compounds in SZ

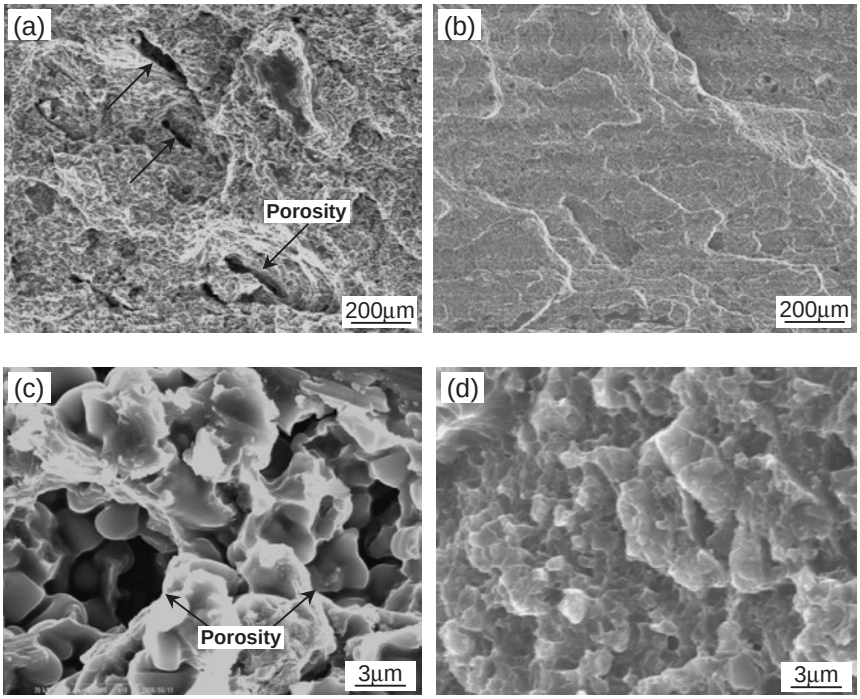

Fig. 11 Fracture surface of tensile samples: (a) BM; (b) SZ; (c) higher magnification of BM; (d) higher magnification of SZ.

decreases with increasing the traveling speed at a constant rotation speed, due to the less heat input.

(3) The hardness of SZ is higher than that of BM, and the tensile strength and elongation both have been improved after FSW, because FSW refines and uniforms the microstructure and intermetallic compounds.

REFERENCES

1) X. Cao, M. Jahazi, J. P. Immarigeon and W. Wallace: J. Mater. Proc. Technol. **171** (2006) 188–204.
2) N. Afrin, D. L. Chen, X. Cao and M. Jahazi: Scr. Mater. **57** (2007) 1004–1007.
3) E. Aghion and B. Bronfin: Materials Science Forum **350–351** (2000) 19–28.
4) K. Nakata, Y. G. Kim, H. Fujii, T. Tsumura and T. Komazaki: Mater. Sci. Eng. A **437** (2006) 274–280.
5) A. L. Etter, T. Baudin, N. Fredj and R. Penelle: Mater. Sci. Eng. A **445–446** (2007) 94–99.
6) C. J. Dawes and W. M. Thomas: Welding J. **75** (1996) 41–45.
7) W. J. Arbegast: Scr. Mater. **58** (2008) 372–376.
8) H. Lombard, D. G. Hattingh, A. Steuwer and M. N. James: Engineering Fracture Mechanics **75** (2008) 341–354.
9) H. B. Chen, K. Yan, T. Lin, S. B. Chen, C. Y. Jiang and Y. Zhao: Mater. Sci. Eng. A **433** (2006) 64–69.
10) R. S. Mishra and Z. Y. Ma: Mater. Sci. Eng. R **50** (2005) 1–78.
11) N. Afrin, D. L. Chen, X. Cao and M. Jahazi: Mater. Sci. Eng. A **472** (2008) 179–186.
12) Z. Y. Ma: Metall. Mater. Trans. A **39A** (2008) 642–658.
13) L. Commin, M. Dumont, J.-E. Masse and L. Barrallier: Acta Mater. **57** (2009) 326–334.
14) G. M. Xie, Z. Y. Ma, L. Geng and R. S. Chen: Mater. Sci. Eng. A **471** (2007) 63–68.
15) W. Blum, P. Zhang, B. Watzinger, B. v. Grossmann and H. G. Haldenwanger: Mater. Sci. Eng. A **319–321** (2001) 735–740.
16) S. Spigarelli, D. Ciccarelli and E. Evangelista: Mater. Lett. **58** (2004) 460–464.
17) K. Nakata, Y. G. Kim and M. Ushio: Trans. JWRI **31** (2002) 141–146.
18) L. Yu, K. Nakata and J. Liao: J. Alloy. Compd. **480** (2009) 340–346.
19) M. M. Avedesian and H. Baker: ASM specialty handbook — Magnesium and Magnesium Alloys, (The Materials Information Society) pp. 37–43.
20) Y. S. Sato, M. Urata and H. Kokawa: Metall. Mater. Trans. A **33** (2002) 625–635.
21) Ø. Frigaard, Ø. Grong and O. T. Midling: Metall. Mater. Trans. A **32** (2001) 1189–1199.
22) Y. G. Kim, H. Fujii, T. Tsumura, T. Komazaki and K. Nakata: Mater. Sci. Eng. A **415** (2006) 250–254.